Phys Chem Minerals (2003) 30: 98 – 107
DOI 10.1007/s00269-002-0292-0

ORIGINAL PAPER

V. M. Khomenko · K. Langer · R. Wirth

On the influence of wavelength-dependent light scattering on the UV-VIS absorption spectra of oxygen-based minerals: a study on silicate glass ceramics as model substances

Received: 15 February 2002 / Accepted: 11 November 2002

Abstract The Mie scattering theory shows that the presence of randomly distributed submicroscopic inclusions with narrow size distribution and a refractive index n_i in a matrix with different refractive index n_m may give rise to a λ-dependent, band-like scattering (e.g., Kortüm 1969). Intensity and spectral position of this scattering depend on a combination of several independent parameters, such as size and number of inclusions, their form and n_i/n_m ratio (Kortüm 1969). Recently, it was confirmed that at a certain inclusion size and n_i/n_m ratio the scattering bands can contribute to the UV-edge in the electronic absorption spectra of garnets, influencing their colour (Khomenko et al. 2001). In natural minerals, however, it is impossible to differentiate between individual influence on scattering of the above mentioned parameters because of complex and interconnected variations in number, size and type of inclusions. Additionally, in most natural minerals variable amounts of transition metal ions are present. They may cause UV-VIS absorption due to ligand to metal charge transfer (LMCT) in the same region where band-like scattering may occur (Khomenko et al. 2001). At least some of these difficulties may be avoided in the case of some glass ceramics where number and size of crystalline microinclusions can be controlled by varying ceramization conditions such that fine-grained homogeneous microstructures are formed (e.g., James 1982; Petzoldt and Pannhorst 1991). Thus, glass ceramics of known composition, containing different amounts of microcrystals of specified size, may serve as unique patterns for the experimental study of effects caused by submicrocrystals on bulk properties of transparent solid materials, such as scattering, UV-VIS transparency and colour. Four types of parent glasses and a series of glass ceramic materials produced from them by heat treatment were investigated using transmission electron microscopy (TEM). These materials were also studied by transmission spectrometry in the range 35 000–20 000 cm^{-1}. Different inclusions, from five to several hundred nm in size, were observed in the glass matrices depending on their compositions and heating history. These inclusions represent two groups: early very small crystals of Ti, Zr oxides and relatively large crystals of stuffed high-quartz type or keatite. The absorption spectra of the glass ceramics show largely varying long-wavelength slopes of the UV absorption. UV-edge intensity correlates mostly with the size of the inclusions and changes drastically when larger keatite-type microcrystals are growing. Small variations in the UV edges also follow the early process of Ti-phase separation and nucleation. This may be explained by Ti depletion from the glass matrix and, thus, by reducing the measured intensity of LMCT in the first co-ordination sphere of Ti^{4+} ions. The different yellowish colourations of unheated glasses studied here are caused by this effect, whereas developing several hundred-nm-large keatite crystals leads to a strong scattering effect and a milky colour in glass ceramics.

Keywords Mie scattering · UV-VIS absorption spectra · Glass ceramics

V. M. Khomenko
Institute of Geochemistry, Mineralogy and Ore Formation,
Ukrainian Academy of Science,
pr. Palladina 34,
252142 Kyiv, Ukraine

V. M. Khomenko · K. Langer
Institut für Angewandte Geowissenschaften I,
Allgemeine und Experimentelle Mineralogie,
Technische Universität Berlin,
Ernst-Reuter-Platz 1,
10623 Berlin, Germany

R. Wirth (✉)
GeoForschungsZentrum Potsdam,
Projektbereich 4.1
Postfach 600751
14407 Potsdam, Germany
E-mail: wirth@gfz-potsdam.de
Tel.: +49 (0331) 288 14 02
Fax: +49 (0331) 288 13 19

Introduction

Absorption spectroscopy in the UV-VIS spectral range has proven its capacity to contribute essentially to the solution of a number of problems in the crystalchemistry and bonding of oxygen-based rock-forming minerals (cf. e.g., abstracts of the IV European Meeting on Absorption Spectroscopy of Minerals Paris 2001). This is true provided the absorption bands in such spectra are properly assigned to the mechanisms giving rise to them.

In this context it is to be recalled that possible influences of wavelength-dependent light scattering, the so-called Mie scattering (Mie 1908; Kortüm 1969), on the spectra, especially on the high-energy absorption edge of oxygen-based minerals, are not yet sufficiently elucidated. Mie scattering leading to band-like features in the spectra, may occur when the matrix of the mineral crystal under study exhibiting the mean refractive index n_m contains submicroscopic inclusions of more or less uniform diameter with a mean refractive index n_i higher or lower than n_m. Inclusions may be minerals, fluid inclusions, inclusions of remnant melt etc.

On the basis of Mie theory (Mie 1908; cf. Kortüm 1969), a general equation connecting intensity of scattered light with physical characteristics of matrix and inclusions can be rewritten in the form:

$$I_S = I_0 \frac{128\pi^5}{3} \frac{Nr^6}{\lambda^4} \left(\frac{m^2 - 1}{m^2 + 2} \right)^2 , \quad (1)$$

where I_S is intensity of scattered light, I_0 the intensity of the primary beam, N the number of inclusions per cm^3, r the radius of inclusion, λ the wavelength and m the relative refractive index n_i/n_m.

Thus, the intensity of scattered light I_S is most strongly dependent on the size of inclusions (variable r), whereas the number of inclusions per volume (their concentration) and refractive indices of matrix and particles (variable m) play less important roles. From Eq. (1), it is also clear that the λ-dependent scattering will drastically enhance its influence in the region of short wavelengths, thus causing bands predominantly in the UV region of the absorption spectrum.

A connection between the transparency of solid materials and presence of microinclusions in their matrices was studied for the case of glass ceramics by Beall and Duke (1969). It was suggested that the transmission is caused by the scattering effect of microcrystals and predominantly determined by their size. Schiffner and Pannhorst (1987) found also that transmission depends on nuclei density. However, in these pioneer studies no quantitative relationships between the transparency in different spectral regions and physical features of microinclusions were investigated. Further, no absorption spectra were reported and no conclusions were drawn concerning changes in optical spectra of glass ceramics caused by λ-dependent, band-like scattering, depending on number, size or refractive index of microcrystals, as well as on composition and refractive index of the matrix. Just these results and their interpretation will be critical for an understanding of the contribution which the scattering effect can make to the absorption spectra of any synthetic and natural materials.

A first study bearing on such phenomena, so far ignored in mineral spectroscopy, was performed on a series of almandine-rich garnets as well as on synthetic almandine and spessartine end members (Khomenko et al. 2001). It turned out that the UV absorption edge of such crystals may indeed contain components due to Mie scattering besides components due to excitation of the oxygen-metal charge transfer.

The aim of the present study is to further elucidate the influence of Mie scattering on the absorption spectra of oxygen-based solid materials. Glass ceramics developed from several parent glasses are used in this study, combining HRTEM and spectroscopic work, because these materials are well known to contain different amounts of microcrystals of definite sizes and compositions and may, therefore, serve as appropriate model substances to show the effects of wavelength-dependent scattering. In addition, by using a two-step development under certain conditions, glass ceramics allow for an independently varying size and number of nuclei and microcrystals (e.g. James 1974; McMillan 1979; Petzoldt and Pannhorst 1991; Beall 1994). Thus, glass ceramics show a broad variety of phenomena bearing on the understanding of the influence of scattering on the absorption spectra of oxygen-based minerals.

Samples and experimental methods

Samples: composition, preparation and treatment

Fragments of four glasses and glass ceramics produced by Schott (Z6, Z7, S and Robax), were cut, ground down to a thickness of ca. 0.2 mm and polished on both sides. All four platelets obtained were divided into several pieces, such that a set of identical smaller platelets with surfaces sized several mm^2 was prepared for each untreated sample. One of the pieces from every set was successively studied using transmission spectroscopy in the UV-VIS region, characterized chemically by electron microprobe techniques and studied by HRTEM. Other pieces were heated gradually in air using the two-step method of ceramization (e.g., Schiffner and Pannhorst 1987; Petzoldt and Pannhorst 1991). After every step of treatment, spectroscopic measurements and TEM investigations were repeatedly carried out on most of the samples. All glass ceramics obtained as final materials after the second step of heating were studied again by means of transmission spectroscopy in the UV-VIS region, electron microprobe techniques and HRTEM. The HRTEM investigations were always carried out on the same platelets which were used in the spectroscopic measurements.

Measurement conditions and standards used for the electron microprobe analyses are described in Langer and Khomenko (1999). Additionally, pure Zn, As and Zr were used as standards for these elements, GaP as a standard for P and $BaSO_4$ as a standard for Ba. All samples studied contain Li and thus differences between 100% and the oxide sums obtained can serve for a rough estimation of Li_2O contents. The chemical compositions of the glasses as mean values of 8 to 16 analyses measured at different points of each sample, are summarized in Table 1. No measurable compositional fluctuations were found in all samples studied. Samples Z6, Z7 and S are characterized by complex composition with presence of Ti and Zr. Both play the role of nucleating agents

Table 1 Composition of glasses studied (wt%) as obtained by electron microprobe analyses. Numbers in parentheses represent standard deviations of the last decimal places quoted. *n.d.* not determined

Sample	Na_2O	MgO	Al_2O_3	SiO_2	P_2O_5	K_2O	CaO	TiO_2	ZnO	As_2O_3	ZrO_2	BaO	Sum[a]
Z6	0.15(3)	1.07(3)	24.97(12)	54.6(11)	7.3(4)	0.60(1)	0.03(1)	1.40(1)	1.42(2)	0.80(8)	1.69(5)	0.00(1)	94.0(12)
Z7	0.13(3)	1.01(2)	24.64(11)	53.1(10)	6.8(4)	0.60(1)	0.02(1)	1.32(1)	1.36(3)	0.76(7)	1.50(6)	0.00(1)	91.2(11)
Robax	0.05(2)	0.00(1)	20.79(11)	71.9(4)	0.00(1)	0.01(1)	0.00(1)	0.00(2)	0.00(1)	n.d.	0.00(3)	n.d.	92.8(5)
S	0.21(4)	1.14(2)	19.57(13)	66.7(14)	0.02(2)	0.20(2)	0.03(0)	2.20(8)	1.67(7)	0.69(7)	1.74(3)	0.82(8)	95.0(2)

[a] Sum deficiencies are due to presence of Li_2O in all four samples

(e.g. James 1982; Petzoldt and Pannhorst 1991). Samples Z6 and Z7 are compositionally very close to Zerodur-type glass ceramics (Schiffner and Pannhorst 1987; Petzoldt and Pannhorst 1991). Robax has a relatively simple composition, predominantly in the system Li_2O–Al_2O_3–SiO_2. Very small amounts of water, bound as OH^- groups, were found in all samples by means of the IR spectroscopic method. These values were evaluated to be ca. 0.02–0.03 mol H_2O l^{-1}, using data of Libowitzky and Rossman (1997).

During treatment, two or three pairs of platelets representing each parent glass sample were heated at the nucleation step at 760–770 °C, one pair for 5, others for 15 and/or 45 min. After this, one of the pieces from each pair was studied by absorption spectroscopy and TEM, and the second was used for further heating at higher temperature, at which crystal growth on nuclei occurs. Temperatures and durations of heating for every sample are summarized in Table 2. Estimated temperature–time errors during heating are ±10 °C and ±1 min. All samples were cooled in air immediately after heat treatment. No experiments with variable cooling rates were carried out.

Absorption spectroscopy

The absorption spectra were measured at room temperature in the spectral range 35 000–20 000 cm^{-1}, i.e., in the near-UV-VIS region, by means of a single-beam microscope spectrometer Zeiss UMSP 80. Ultrafluars 10x served as objective and condenser. The reference spectra were measured in air. The diameter of the measuring spot was 32 μm, the spectral slit width and step width were both 2 nm. Further experimental details are given in Langer (1988). The errors in the linear extinction coefficients, extracted from the measured spectra at 30 000 and 25 000 cm^{-1} (Table 2), are estimated to be not greater than 2%.

Several absorption spectra of starting glasses and treated ceramics were measured at crossed polarizers between 28 000 and 15 000 cm^{-1} as an independent check for the presence of microinclusions. A detailed description of this method and measuring procedure is presented in Khomenko et al. (2001).

High-resolution TEM study

The same platelets of glass ceramics on which absorption spectra were measured later were used for the electron microscopy investigation. Samples for TEM were prepared using the standard ion beam thinning technique. Carbon coating prevents charging of the samples in the electron microscope. Specimens were investigated with a Philips CM200 electron microscope operated at 200 kV and equipped with a LaB_6 filament as electron source. HRTEM images were acquired as energy-filtered images by applying a 10-eV win-

Table 2 Colours of glasses and glass ceramics studied and their linear extinction coefficients in the near-UV and VIS spectral regions as extracted from the absorption spectra at 30 000 cm^{-1} and 25 000 cm^{-1}, respectively

Sample	Colour of mm-thick platelets in transparent light	Linear extinction coefficient, (cm^{-1})	
		$k_{30\,000}$	$k_{25\,000}$
Z6			
Unheated	Colourless	3	1.4
760 °C × 5′	Colourless	2	0.9
760 °C × 15′	Colourless	2.1	1.0
760 °C × 45′	Colourless	2.7	1.1
760 °C × 5′ + 900 °C × 30′	Milky yellowish white	55.2	21.3
760 °C × 15′ + 900 °C × 30′	Light milky yellow	29.8	6.1
760 °C × 45′ + 900 °C × 30′	Colourless	44.8	0.7
Z7			
Unheated	Colourless	6.6	1.4
760 °C × 5′	Colourless	5.7	0.7
760 °C × 15′	Colourless	5.6	0.4
760 °C × 45′	Colourless	7.9	1.2
760 °C × 5′ + 900 °C × 30′	Colourless	41.3	0.8
760 °C × 15′ + 900 °C × 30′	Colourless	42.5	1.0
760 °C × 45′ + 900 °C × 30′	Colourless	40.2	1.6
S			
Preheated	Light yellow	79.5	2.2
760 °C × 5′	Light yellow	79.1	1.8
760 °C × 45′	Light yellow	79.8	2.1
760 °C × 5′ + 900 °C × 40′	Light yellow	83	1.8
760 °C × 45′ + 900 °C × 40′	Light yellow	75.3	1.6
980 °C × 100′	Light orange	180	14
Robax			
Unheated	Colourless	2.9	0.7
770 °C × 420′	Colourless	23.6	10.8

dow to the zero-loss peak (Gatan Imaging Filter, GIF). The chemical composition was determined by analytical electron microscopy (AEM) using an EDAX X-ray analyzer with ultrathin window. The spectra were recorded for 200 s to achieve reasonable counting statistics. All spectra were corrected for absorption and fluorescence. The foil thickness necessary for the correction was determined by electron energy-loss spectroscopy (EELS) using the total intensity of the electrons reaching the EEL spectrometer and the intensity of the zero-loss peak (Egerton 1996).

Several TEM images (1000×1000 nm) were obtained for all samples studied and the mean number of inclusions cm^{-3} of glassy matrix was calculated in every case by applying a foil thickness of 100 nm. Additionally, observations of ceramic development in situ were performed during heating experiments. These were carried out on glass Z7 at temperatures of 640, 740 and 890 °C directly in TEM.

Results

Inclusions and their characterization by HRTEM techniques

The starting glasses Z6, Z7 and Robax show no inclusions even at very high magnifications; their diffraction patterns exhibit only the characteristic diffuse scattering intensity of an amorphous phase. Thus, they can be regarded as base glasses. In contrast, the starting sample S reveals a ceramic structure. It contains abundant small inclusions homogeneously distributed in the matrix. Most of them are isometric, strongly enriched in Ti, with an average radius of about 20 nm. Their lattice parameters suggest that they are brookite crystals. No differences in type, size or number of inclusions compared to the starting S ceramic were found after it was heated for 45 min at 760 °C. This confirms that the sample was already treated at nucleation temperature.

In pieces of Z6 and Z7, which were heated at 760 °C for 5 min, no crystals were found, but Ti-rich areas about 5 nm in diameter with another mass absorption contrast were observed in Z7 (Fig. 1a, b). This supports the conclusion concerning phase separation, which precedes nucleation in similar glasses (Petzoldt and Pannhorst 1991). On heating Z6 in situ in TEM, the first tiny TiO_2 inclusions appeared already after 3 min at 740 °C, but the nucleation occurred inhomogeneously at this temperature and most of the Z6 matrix did not show any inclusions. After 45 min heating, Z7 and Z6 show randomly distributed very small crystals of TiO_2 phase, probably rutile, and some Zr-enriched crystals, both less than 10 nm. No large inclusions were observed.

Robax glass contains no nucleating agents like Ti or Zr oxides and, therefore, exhibits a ceramization pattern different from the above mentioned materials. After heating at 770 °C, relatively large crystals up to 150–200 nm in diameter and of the same composition as the glass matrix were detected. These high-quartz or keatite crystals are distributed inhomogeneously, alternating in the matrix with crystal-free areas.

Sample S, heated for 60 min at 1000 °C after 45 min preheating at 760 °C, contains two main sets of randomly distributed inclusions (Fig. 2a, b). The elemental maps show that Ti and Zr are associated with very small crystals of radii 20–35 nm (Fig. 3), whereas Zn enriches larger particles, sometimes several hundred nm in diameter (Fig. 2b). Small crystals contain either both Ti and Zr or only Ti (Fig. 3); they were identified as Ti–Zr and Ti oxides, respectively. Zn usually contributes to the formation of the stuffed keatite-type crystals (Petzoldt and Pannhorst 1991).

Two sets of inclusions, similar to those found in sample S, are observed after two heating steps also in glass ceramics Z6 and Z7. The inclusions are represented by small crystals of 10–15 nm in diameter, which are Ti- or Zr-rich oxide phases, and by larger keatite-type crystals. HRTEM images were used to calculate diffraction patterns of the Zr-rich inclusion. The obtained data showed that the inclusions are ZrO_2 crystal. The main distinction between the glass ceramics developed from the

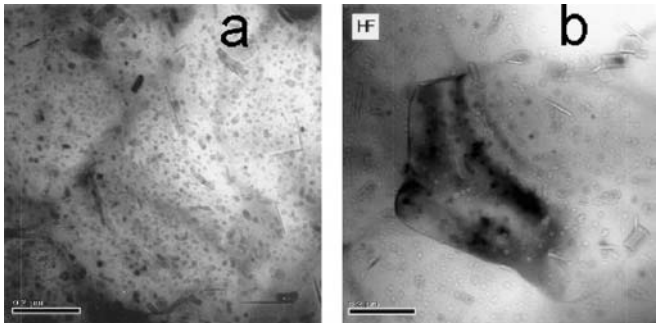

Fig. 2a, b TEM bright-field images of S ceramic heated for 60 min at 1000 °C after preheating at 760 °C for 45 min. **a** Randomly distributed small crystals. **b** Large crystal

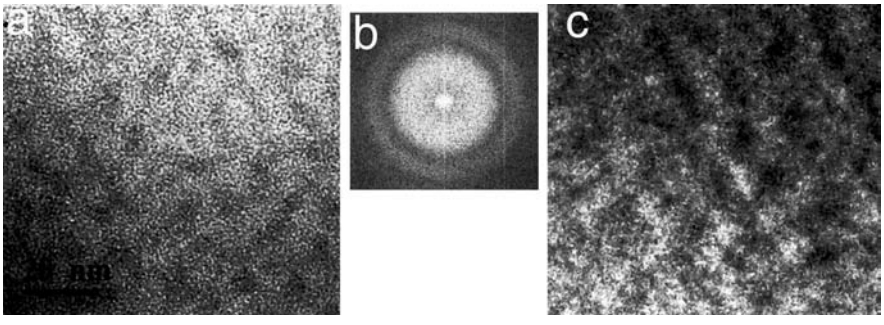

Fig. 1a–c TEM characterization of Z7 glass heated at 760 °C for 5 min. **a** Bright-field image. The *dark areas* about 5 nm in diameter show another mass absorption contrast. **b** Diffraction pattern exhibiting the characteristic diffuse scattering of an amorphous phase. **c** Ti elemental map indicating Ti enrichment of the dark areas of **a**

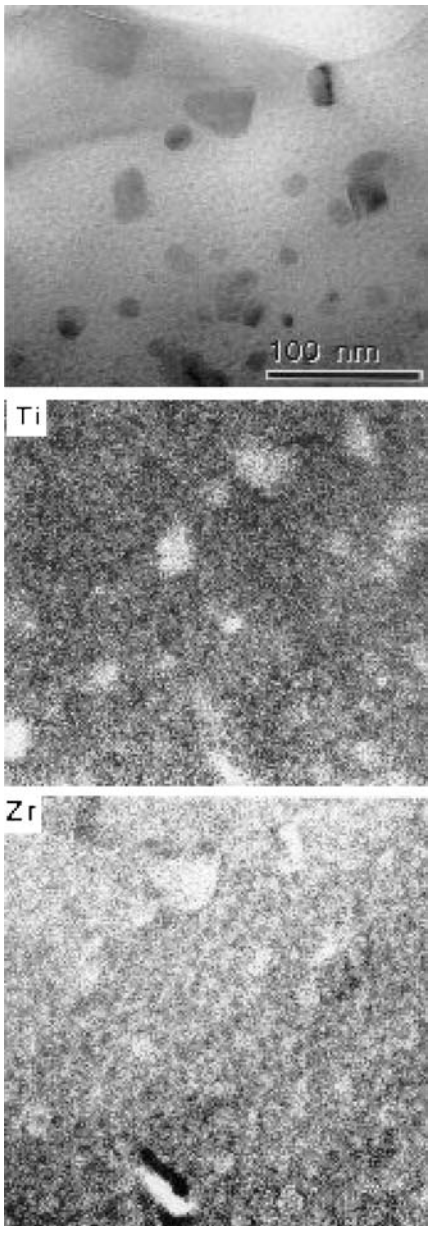

Fig. 3a–c TEM characterization of Ti- and Zr-oxide microcrystals in S ceramic developed in two-step treatment. **a** Bright-field image. **b** Ti elemental map of the same area. **c** Zr elemental map of the same area

same samples in different runs of two-step heating is the variation in size and number of both types of inclusions depending on preheating duration (Fig. 4; Table 3). An overview of the inclusions found, their concentration, composition, as well as some optical properties, is listed in Table 3.

Absorption spectra

Absorption spectra of the starting glasses and the developed glass ceramics show strong differences in their UV-absorption edges (Fig. 5). Robax glass shows the lowest absorption through the whole measured spectral

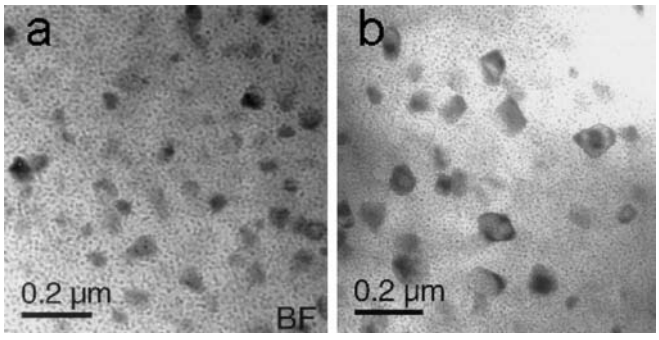

Fig. 4a, b TEM bright-field images showing different size of keatite-type crystals in Z7 ceramics developed in two-step treatment after preheating at 760 °C for 5 min **a**, and 45 min **b**

range. The reason may be the absence of Ti in this sample and, hence, the absence of LMCT bands originating from electronic transitions in Ti^{4+}–O_n clusters (e.g., Tossel et al. 1973; Marfunin 1979), In its spectrum. The highest UV absorption demonstrates glass ceramic S. This sample is characterized by the presence of abundant small inclusions (Fig. 2a; Table 3) and by the highest Ti content (Table 1). Both factors intensify UV absorption due to scattering effect and LMCT, respectively (Khomenko et al. 2001).

Absorption spectra of glass ceramic S, measured after preheating at 760 °C for 5 and 45 min nearly coincide with a spectrum of the starting material (Fig. 6). In contrast, spectra of preheated Z6 and Z7 glasses demonstrate distinct differences if compared with spectra of the corresponding unheated glasses: after 5 and 15 min treatment, UV absorption decreases in both samples, whereas after 45 min heating, UV absorption increases, even above its initial value, in starting Z7 glass (Fig. 6; Table 2). This complex behaviour can be connected with Ti segregation in very small Ti-enriched areas, which appear during the first minutes of preheating (Fig. 1), and with further nucleation of small TiO_2 crystals. Perhaps depletion of the matrix in Ti leads to decrease of LMCT band in the UV. Later, nucleation of small crystals causes λ-dependent scattering, which, in turn, intensifies the UV edge.

Spectra of glass ceramics developed after heating at 900 °C from the samples preheated for different times, are shown in Fig. 7. Only minor variations in the UV-edge intensities can be found in spectra of S and Z7 samples depending on preheating time, whereas the spectra of Z6 ceramics indicate complex changes in UV-VIS regions. To evaluate changes in intensity and/or spectral position of the UV edge, the linear extinction coefficient at 30 000 cm^{-1} was used, because any low-energy shift of the UV edge will result in an increasing linear absorption coefficient at any wavenumber in the UV slope of the respective spectrum. By analogy, the linear extinction coefficient at 25 000 cm^{-1} was used as a measure of absorption in the visible (blue) spectral range. These two values, listed in Table 2, reflect the

Table 3 Characterization of microinclusions in glass ceramics as identified by TEM study. n.d. – not determined

Sample	Inclusions	Number (cm^{-3})	Mean radius (nm)	Refractive indexes[a] (n)		$m = n_i/n_m$	UV absorption
				Matrix (n_m)	Inclusion (n_i)		
Z6							
Unheated	No	–	–	1.53	–	–	–
760 °C × 5′	No	–	–	1.53	–	–	–
760 °C × 45′	TiO_2	n.d.	4	1.53	2.7	1.8	Strong
760 °C × 5′ + 900 °C × 30′	TiO_2, ZrO_2	1.5×10^{16}	10	1.54	2.7, 2	1.8, 1.3	Strong
	Keatite	2×10^{12}	600	1.54	1.5	1.02	Low
760 °C × 15′ + 900 °C × 30′	TiO_2, ZrO_2	2×10^{16}	10	1.54	2.7, 2	1.8, 1.3	Strong
	Keatite	10^{14}	200	1.54	1.5	1.02	Low
760 °C × 45′ + 900 °C × 30′	TiO_2, ZrO_2	3×10^{16}	15	1.54	2.7, 2	1.8, 1.3	Strong
	Keatite	2×10^{15}	50	1.54	1.5	1.02	Low
Z7							
Unheated	No	–	–	1.53	–	–	–
760 °C × 5′	No	–	–	1.53	–	–	–
760 °C × 45′	TiO_2	n.d.	5	1.53	2.7	1.8	Strong
760 °C × 5′ + 900 °C × 30′	TiO_2, ZrO_2	2.5×10^{16}	10	1.54	2.7, 2	1.8, 1.3	Strong
	Keatite	2×10^{12}	25	1.54	1.5	1.02	Low
760 °C × 45′ + 900 °C × 30′	TiO_2, ZrO_2	3×10^{16}	10	1.54	2.7, 2	1.8, 1.3	Strong
	Keatite	2×10^{15}	60	1.54	1.5	1.02	Low
S							
Preheated	TiO_2	6×10^{15}	20	1.55	2.7	1.8	Strong
980 °C × 60′	TiO_2, $ZrTiO_4$	5×10^{15}	25	1.55	2.7	1.8	Strong
	Keatite	2×10^{14}	400	1.55	1.5	1.03	Low
Robax							
Unheated	No	–	–	1.51	–	–	–
770 °C × 420′	Keatite	2×10^{15}	150	1.51	1.5	1.01	Low

[a] Refractive indices estimated on the basis of published data summarized in Tröger (1971)

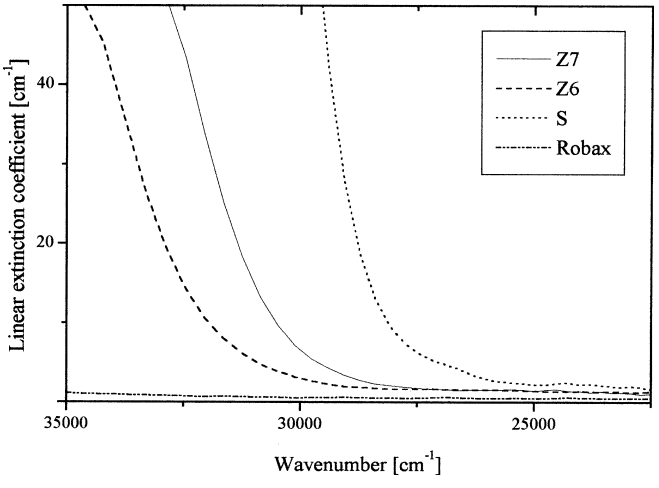

Fig. 5 UV-VIS absorption spectra of starting glass materials

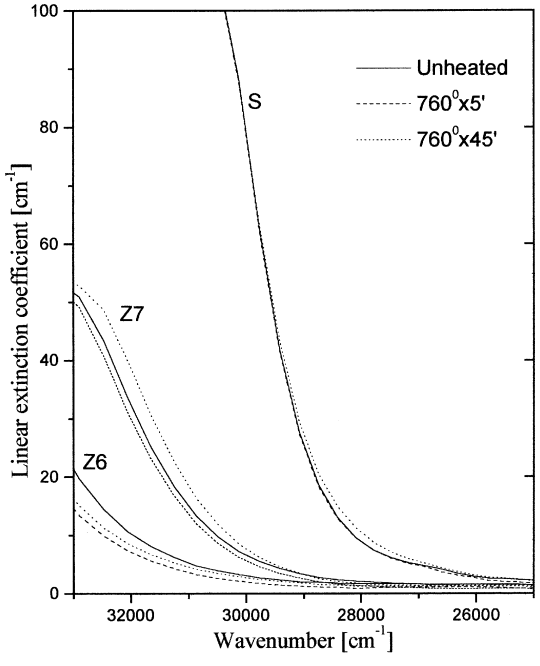

Fig. 6 Absorption spectra of S, Z6 and Z7 samples before and after heating at 760 °C for 5 and 45 min

shape of the measured absorption spectra of glass ceramics (cf. Table 2 and Fig. 7).

Spectra of starting materials and ceramics obtained from samples S and Z6 were measured also at crossed polarizers (Fig. 8). Zero remnant intensity is typical of inclusion-free materials, whereas the slight deviations towards excess intensity are within the limitation of this method (Khomenko et al. 2001). The resulting spectra lie slightly above the zero line in the region 27 000–15 000 cm^{-1} in the case of starting glasses, as well as in the case of glass ceramics containing microcrystals sized less than 100 nm. Only spectra of those glass ceramics which contain larger inclusions, such as Z6 preheated for 5 or 15 min and S heated at 980 °C, lie below the zero line, indicating lightening in the visible region due to the presence of inclusions (cf. Fig. 8 and Table 3).

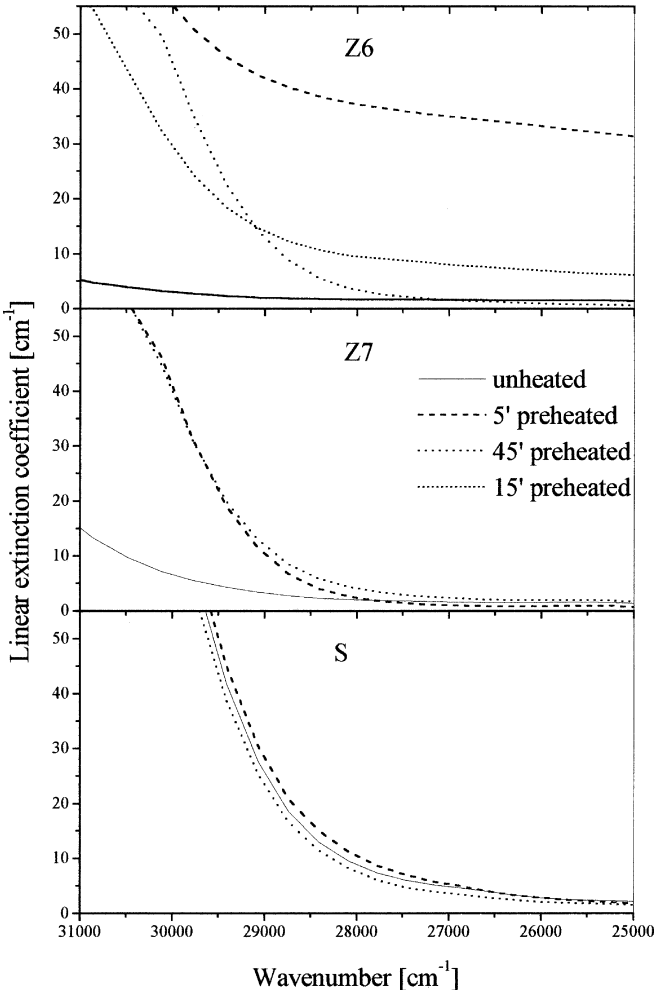

Fig. 7 Absorption spectra of S, Z6 and Z7 ceramics developed in two-step treatments with different preheating times at 760 °C

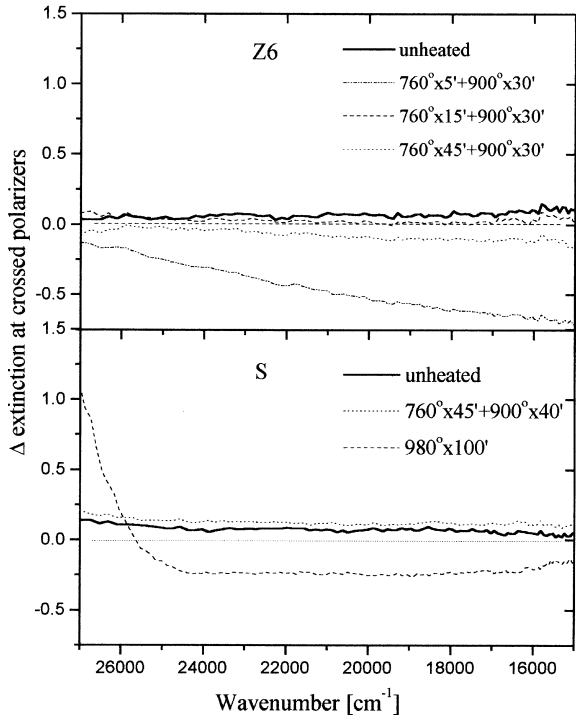

Fig. 8 Spectra of extinction difference measured at crossed polarizers on Z6 and S samples before and after heating

Evaluation of experimental data and conclusions

Intensity of UV-scattering: roles of size and concentration of inclusions

Data listed in Tables 2 and 3 show that variations in type, size and number of microinclusions in glass ceramic samples induce strong changes in their UV-VIS absorption spectra. At the same time, the respective EELS spectra confirm that in each glass ceramic series derived from the same parent glass, the composition of the matrix does not change significantly. Moreover, the most important depletion of the matrix in the nucleating agents Ti and Zr takes place during the separation and nucleation stages, when absorption spectra show only minor changes (Fig. 6). Thus, inclusions play a dominant role in the bulk UV-VIS absorption of these ceramics. The intrinsic absorption of inclusions, however, contributes only negligibly because of their size ($\ll\lambda$) in the case of Ti, Zr oxides, and because of low UV-VIS absorption in the case of relatively large keatite-type crystals. Therefore, scattering is the main cause of the UV-VIS edge in the absorption spectra of the glass ceramics studied.

Glass ceramics developed from different parent glasses by similar procedures show broad variations in both absolute values of linear extinction coefficients measured in different spectral regions and in their proportion (Fig. 7, 9). This observation should be connected with characteristics of inclusions in the respective ceramics. As obvious from Eq. (1), the size of inclusions, their concentration in the matrix and their refractive indices are the main factors influencing scattering. Further, Mie theory predicts a linear correlation between the maximum of the Mie function (wavelength of maximal scattering λ) and the radius of inclusion at every constant relative refractive index m (e.g., Mie 1908; Kortüm 1969). Taking into account that in most samples studied here, there are two main kinds of inclusions which demonstrate great differences in geometrical and physical parameters (Table 3), independent variations in the UV and visible parts of spectra may reflect the influences of these different types of inclusions.

Indeed, all ceramics derived from the samples studied after preheating at 760 °C, as well as all Z7 ceramics, show a definite increase in UV absorption measured at 30 000 cm^{-1}, but very small variations in the visible region at low linear extinction coefficient values (< 2.5 cm^{-1}) (Fig. 9). These samples contain either only small Ti-, Zr-oxide inclusions, or, in addition, also the keatite-type inclusions, as in the case of Z7 ceramics heated at 900 °C (Table 3). The latter, however, are relatively

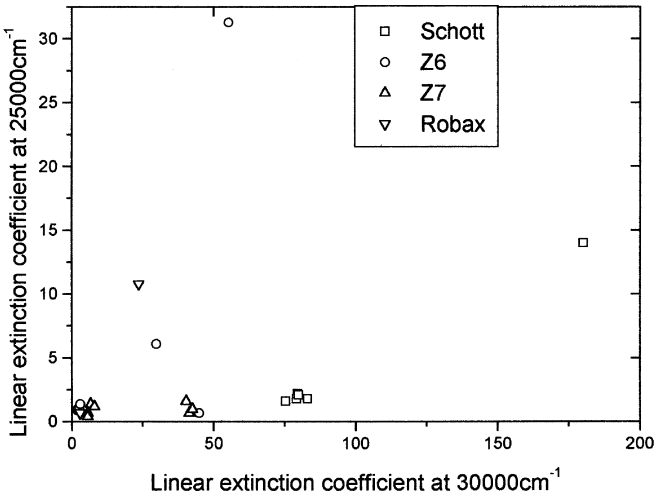

Fig. 9 Dependence between linear absorption coefficients measured at 30 000 and 25 000 cm^{-1} in the spectra of glasses and the glass ceramics studied

small, with radii less than 100 nm. In contrast, ceramics Z6 and S heated at 900 or at 980 °C, as well as Robax ceramic heated at 770 °C, demonstrate a strong increase of absorption also in the visible region if compared to the respective unheated and preheated materials (Fig. 9). All these ceramics contain relatively large keatite-type crystals, more than 150–200 nm in diameter (Table 3). Thus, small inclusions influence the intensity of λ-dependent scattering in the UV region, whereas larger inclusions cause a scattering effect also in the visible. The latter effect can be observed in respective absorption spectra as an increase of the linear extinction coefficient at 25 000 cm^{-1} (Figs. 7, 9).

Khomenko et al. (2001) described a procedure which allows the evaluation of spectral positions of the band-like scattering maxima for known m and r values on the basis of the Mie theory. Such a calculation shows that the Mie function will have a strong maximum in far-UV at $\lambda = 30$–80 nm in the case of small TiO_2 inclusions in the ceramics studied. This means that wings of scattering bands connected with such inclusions can mostly influence the position of the UV edge in the absorption spectra, whereas their contribution to the visible spectra is negligible. A rough estimation of the spectral position of a broad scattering maximum caused by large keatite inclusions in glass ceramics gives 150–300 nm. It corresponds to 65 000–33 000 cm^{-1} and thus can cause a low-energy wing to spread the respective absorption edge into the visible spectral region. In the UV, the influence of larger keatite inclusions should be much less than that of Ti oxides because of the difference in their concentration (Table 3), but also because of the strong difference in relative refractive index (cl. Kortüm 1969).

Taking into account the above estimations, we can try to discriminate between influences of different characteristics of inclusions on the absorption caused by λ-dependent scattering. For this, we analyzed the relations between properties of the larger keatite-type inclusions with predominant absorption at 25 000 cm^{-1}, whereas characteristics of Ti-oxide inclusions were used to establish relations with UV edge intensity measured at 30 000 cm^{-1}. In this way, strong correlations were found in both cases between sizes of inclusions and linear extinction coefficients in the respective spectral regions (Fig. 10a, b).

At the same time, a slight correlation between the concentration of inclusions and extinction intensities can be observed only when samples containing equal-sized inclusions are considered. When samples bearing inclusions of different sizes are shown on the same graph, the correlation between inclusion concentration and extinction will be destroyed due to the predominant influence of the size factor (cf. Fig. 10c; Table 3). The results of this study also do not indicate a clear correlation between relative refractive index m and scattering intensity. However, by analyzing Eq. (1), it can be concluded that variable m will play only a minor role in scattering intensity if compared to the influence of the size and concentration of the inclusion.

Refractive indices and UV scattering

The refractive indices of the glass ceramics studied change typically after heat treatment: they increase slightly compared to the starting glasses (Table 3). Measurements in a standard Topcon refractometer provide bulk refractive indices of glass ceramics which are, in fact, very close to indices of parent glasses and thus were taken as matrix indices in our study. However, refraction is a bulk property and can be influenced by the presence of homogeneously distributed microinclusions in the case of glass ceramics. A classical theory of optics includes the Helmholz equations, which relate the refractive index with the spectral position, width and intensity of strong absorption bands in the UV (e.g., Strens 1967). This concept is valid for transparent minerals and also for the glass ceramics studied: there is a clear correlation between their refractive indices and the respective linear extinction coefficients measured in the UV at 30 000 cm^{-1} (Fig. 11). The latter, in turn, are strongly dependent on the sizes of the TiO_2 submicro-inclusions, as shown above.

Conclusions

The results obtained here on glass ceramics prove the applicability of the Mie theory of scattering for the interpretation of UV-VIS spectra of minerals and other solid materials containing microinclusions. Ceramics bearing microcrystals of specified types and sizes were used as model substances for the experimental study of effects caused by Mie scattering on optical spectra and bulk properties of transparent solid materials. Thus, the following conclusions can be applied in mineralogy, as

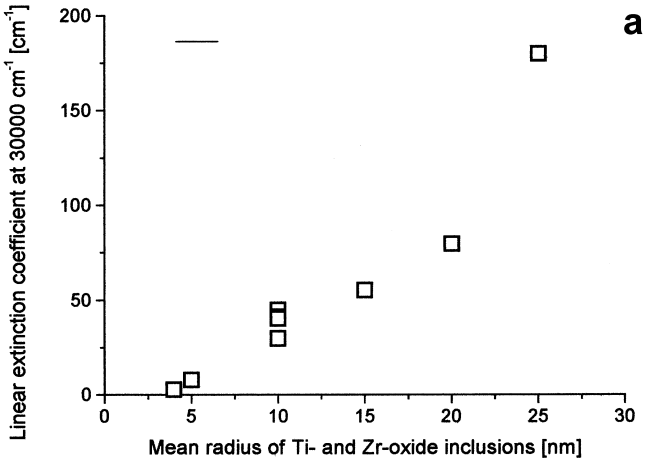

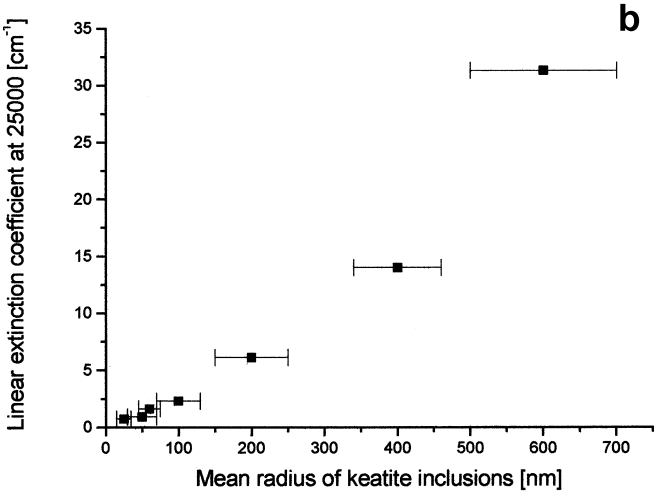

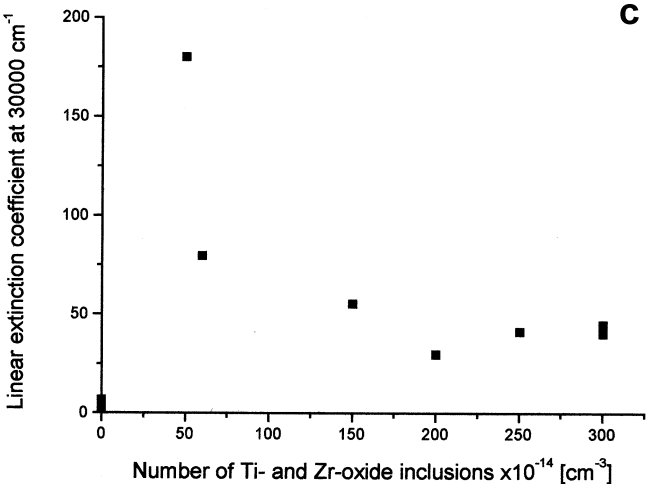

Fig. 10a–c Correlations between linear extinction coefficients measured in different parts of the absorption spectra of glass ceramics and mean radius or number of inclusions in respective ceramic matrices. **a** Correlation between linear extinction coefficients measured in UV at 30 000 cm^{-1} and mean radius of Ti-, Zr-oxide inclusions. **b** Correlation between linear extinction coefficients measured in UV at 30 000 cm^{-1} and number of Ti-, Zr-oxide inclusions. **c** Correlations between linear extinction coefficients measured in VIS at 25 000 cm^{-1} and mean radius of keatite inclusions

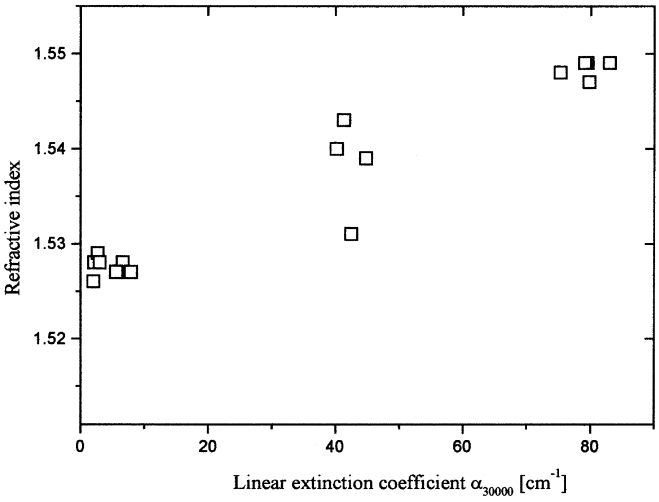

Fig. 11 Correlation between bulk refractive indices of glass ceramics and their linear extinction coefficients measured in UV at 30 000 cm^{-1}

well as in other fields of material science and engineering.

Strong band-like λ-dependent scattering plays a dominant role in the absorption spectra of the glass ceramics studied, determining their shapes and intensities in the UV and visible regions. LMCT bands cause slight differences in the position of the UV-absorption edges only in the spectra of the inclusion-free Ti-bearing glasses. According to the Mie functions, the position of the scattering maximum depends on both relative refractive index m and the size of the inclusion, and occurs typically in the far-UV, as in the case of TiO_2 microinclusions in the ceramics studied. The low-frequency wing of such band-like scattering spread into the near-UV region, influencing the optical spectra. The role of scattering in the absorption spectra in the visible region is limited. However, in the case of a relatively large size of inclusions ($n \times 10^2$ nm) and low m value, the scattering maximum occurs in the near-UV, exerting a strong influence on the blue part of the visible spectral region and, hence, on the colour of inclusion-bearing materials. This is typical of ceramics containing keatite crystals several hundred nm in diameter.

The intensity of the band-like scattering depends predominantly on the size of the inclusions. The number of inclusions, as well as the relative refractive indices, plays a secondary role. Strong correlation between inclusion sizes and extinction coefficients, measured at a certain wavenumber, can be of practical interest, serving to evaluate the size of the submicrocrystals in both natural minerals and artificial materials with defined types of inclusions.

Bulk refractive indices of ceramics show a correlation with the intensities of their UV absorption and, therefore, also with mean inclusion sizes.

Acknowledgements M. Garsche and A. Kisljuck generously provided the base glass and glass ceramic samples. F. Galbert and S. Herhing-Aghte, both at the Technical University Berlin, helped with electron microprobe analyses and refractive indices measurements, respectively. The Deutsche Forschungsgemeinschaft, Bonn-Bad Godesberg, provided financial support through grant La324/35. To all these individuals and this institution our sincere thanks are due.

References

Abstracts of IV European Meeting on Absorption Spectroscopy of Minerals, Paris 2001 (2001). In: Bulletin de liaison de la Societe Francaise de Mineralogie et de Cristallographie 13, N3: 57–116

Beall GH (1994) Industrial applications of silica. In: Reviews in Mineralogy, vol. 29: Silica – Physical Behavior, Geochemistry and Materials Application. Heaney PJ, Prewitt CT, Gibbs GV eds. Mineralogical Society of America, Washington, DC, pp 468–505

Beall GH, Duke DA (1969) Transparent glass ceramics. J Mater Sci 4: 340–352

Burns RG (1993) Mineralogical applications of crystal field theory, 2nd ed. Cambridge Univ Press, Cambridge

Egerton RF (1996) Electron energy-loss spectroscopy in the electron microscope. Plenum New York, pp 301–312

James (1974) Kinetics of crystal nucleation in lithium silicate glasses. Phys Chem Glasses 15: 95–105

James (1982) Nucleation in glass-forming systems—a review. In: Simmons JH, Uhlmann DR, Beall GH (eds) Nucleation and crystallization in glasses. Columbus, Ohio, pp 1–48

Khomenko VM, Langer K, Wirth R, Weyer B (2001) Mie scattering and charge transfer phenomena as causes of the UV edge in the absorption spectra of natural and synthetic almandine garnets. Phys Chem Miner 29: 201–209

Kortüm G (1969) Reflexionsspektroskopie. Springer, Berlin Heidelberg New York

Langer K (1988) UV to NIR spectra of silicate minerals obtained by microscope spectrometry and their use in mineral thermodynamics and kinetics. In: Salje EKH (ed) Physical properties and thermodynamic behaviour of minerals. Reidel, Dordrecht, pp 639–685

Langer and Khomenko (1999) The influence of crystal field stabilization energy on Fe^{2+} partitioning in paragenetic minerals. Contrib Mineral Petrol 137: 220–231

Libowitzky E, Rossman GR (1997) An IR absorption calibration for water in minerals. Am Mineral 82: 1111–1115

Marfunin AS (1979) Physics of minerals and inorganic materials. Springer, Berlin Heidelberg New York

McMillan PW (1979) Glass ceramics, 2nd ed. Academic Press, London

Mie G (1908) Beiträge zur Optik trüber Medien, speziell kolloidaler Gold Lösungen. Ann Phys 25: 377–445

Petzoldt J, Pannhorst W (1991) Chemistry and structure of glass-ceramic materials for high precision optical applications. J Non-Cryst Solids 129: 191–198

Schiffner U, Pannhorst W (1987) Nucleation in a precursor glass for a Li_2–Al_2O_3–SiO_2 glass ceramic, part 1. Nucleation kinetics. Glastech Ber 60: 211–221

Strens RGJ, Freer R (1978) The physical basis of mineral optics I. Classical theory. Mineral Mag 42: 19–30

Tossel JA, Vaughan DJ, Johnson KH (1973) The electronic structure of rutile, wustite, and hematite from molecular orbital calculations. Am Mineral 59: 319–334

Tröger WE (1971) Optische Bestimmung der Gesteinsbildenden Minerale. E. Schweizer bart'sche Verlagsbuchhandlung, Stuttgart